



The usefulness of full-iterative reconstruction algorithm for the visualization of cystic artery on CT angiography

Toshihiko Hamamura¹ · Yoshiko Hayashida¹ · Yohei Takeshita¹ · Koichiro Sugimoto¹ · Issei Ueda¹ · Koichiro Futatsuya¹ · Shingo Kakeda¹ · Takatoshi Aoki¹ · Yukunori Korogi¹

Received: 29 January 2019 / Accepted: 8 April 2019 / Published online: 30 April 2019
© Japan Radiological Society 2019

Abstract

Purpose To evaluate the potential of full-iterative reconstruction (IR) for improving image quality of the cystic artery on CT angiography and to assess observer performance.

Methods Thirty patients who underwent both liver dynamic CT and conventional angiography were included in this retrospective study. All CT data were reconstructed through filtered back projection (FBP), adaptive iterative dose reduction 3D (AIDR3D), and forward-projected, model-based, iterative reconstruction solution (FIRST), respectively. In objective study, we analyzed mean Δ CT numbers (the difference between the HU peak of the vessel and the background) and full-width at tenth-maximum (FWTM) of three parts of the cystic artery by profile curve method comparing the three reconstructions. Subjectively, visualization was evaluated using a four-point scale performed by two blinded observers. ANOVA was used for statistical analysis.

Results In all parts of the cystic artery, the mean Δ CT number of FIRST was shown to be significantly better than that of FBP and AIDR3D ($p < 0.05$). FWTM in FIRST was the smallest in all of the vessels. The mean visualization score was significantly better with FIRST than with other CT reconstructions ($p < 0.05$).

Conclusions The FIRST algorithm led to improved CTA visualization of the cystic artery.

Keywords Iterative reconstruction · Cystic artery · Computed tomography angiography · Image quality

Introduction

The cystic artery originates typically from the right hepatic artery; however, anatomical variations of the cystic arteries (e.g., variation of origin or the number of the arteries) are not uncommon in the general population [1, 2]. Trans-arterial chemoembolization (TACE) has been demonstrated to be an efficient treatment option in patients with advanced hepatocellular carcinoma (HCC). However, embolic materials exhibit a potential risk of cholecystitis and biliary complications considered to be the result of inadvertent embolization of the cystic artery. It was observed more often using drug-eluting beads compared with conventional TACE [3]. Currently, laparoscopic cholecystectomy (LC) is a gold

standard treatment for cholelithiasis. It has been noted that the risk of injury during LC is significantly higher than open cholecystectomy. Anatomical variation of the cystic arteries within Calot's triangle has been reported at 23.4–37.6% and it may be the cause of one of the most dangerous complications; bleeding in the hepatobiliary triangle [4, 5]. Therefore, radiologists and surgeons have been interested in gallbladder vascularization for TACE and LC, since preoperative identification of cystic arteries would allow avoidance of accidental complications [4, 5].

Multidetector-row computed tomography angiography (CTA) is a suitable noninvasive imaging modality for understanding peripheral vessels. Since the inception of the modality, the filtered back projection (FBP) algorithm has been used for reconstruction of CT images from raw data. The detection of the cystic artery by CTA still presents a challenge. This may be due to the lack of enough injection pressure of contrast materials toward to such small diameter arteries. To visualize the cystic artery clearly and accurately,

✉ Toshihiko Hamamura
t-hamamura@med.uoeh-u.ac.jp

¹ Department of Radiology, University of Occupational and Environmental Health, 1-1 Iseigaoka, Yahatanishi-ku, Kitakyushu 807-8555, Japan

we may require applying higher injection pressure, such as trans-arterial angiography.

CT images reconstructed using iterative reconstruction (IR) may provide substantially less image noise from the same raw data through more complex modeling of detector response and of the statistical measurements. Recently, hybrid IR and full IR technique have become available for clinical use. Hybrid IR uses an adaptive shortcut for iterative reconstruction after a first-pass FBP reconstruction. Therefore, hybrid IR can help shorten the longer reconstruction time of pure iterative reconstruction providing much lower image noise than that with FBP alone. Adaptive iterative dose reduction (AIDR) 3D (Canon Medical Systems, Tochigi, Japan) is one of a hybrid IR techniques used in 320-row CT. More recently, a much more complex iterative reconstruction algorithm, referred to as full-model-based iterative reconstruction (Full IR), has become available. Forward-projected, model-based, iterative reconstruction solution (FIRST; Canon Medical Systems, Tochigi, Japan), which is one of the full IR algorithms, has been also released [6–9].

Several recent studies [10–15] reported that full IR technique might improve the image quality and spatial resolution and reduce image noise more than widespread CT reconstruction algorithms, such as FBP or hybrid IR. For CT angiography, the usefulness of the full IR technique has been reported for delineating small vascular structures. However, there were few studies to assess abdominal vessels. Furthermore, to our knowledge, no study has evaluated the feasibility and capability of the full IR technique for the small diameter abdominal arteries, such as the cystic arteries compared to invasive abdominal angiography.

The objective of this retrospective study was to evaluate the potential of full IR for improving image quality of the cystic artery on CTA and to assess the observer performance of each CT reconstruction algorithm.

Materials and methods

Subjects

The study population consisted of 30 consecutive patients (mean age 72.0 years; range 57–89 years) who had undergone both liver dynamic CT and conventional angiography for the TACE of HCC from August 2016 to March 2017. The mean time interval between dynamic CT and angiography was 64 days (from 1 to 190 days). We used conventional angiography as a gold standard for evaluating the cystic artery. The study was approved by our institutional review board, and the requirement for informed consent had been waived.

CT data acquisition and reconstruction

All CT examinations were performed using a 320-ADCT scanner (Aquilion ONE; Canon Medical Systems, Tochigi, Japan). All CT data were acquired using the following parameters: tube voltage, 120 kV; gantry rotation speed, 0.5 s; collimation, 80×0.5 mm; and beam pitch, 0.813. Automatic exposure control with a fixed noise index (SD 8 at 3 mm thickness) was used for tube current.

IV contrast medium (550 mg I/kg body weight) was administered at a rate of 3 mL/s using a double-headed power injector (Dual Shot-Type GX7; Nemoto-kyorindo, Tokyo, Japan). An automatic bolus-tracking technique was used to initiate the early arterial phase scan after the injection of contrast material.

The automatic dose-report displayed a mean volume CT dose index (CTDI vol) of 17.5 mGy and a mean dose-length product (DLP) of 536.2 mGy×cm.

The helical data were reconstructed using FBP and AIDR3D (mild setting) with our standard reconstruction kernel (FC14), and FIRST with a section thickness of 0.5 mm, intervals of 0.4 mm, and a field of view of 320–400 mm. The FIRST method did not include filter kernels; rather, different parameters were set depending on the clinical application, e.g., body, bone, and lung. In this study, we used a clinically optimized parameter, “body” for FIRST (standard setting).

Quantitative image analysis

Quantitative measurements of the CT images were performed with the use of profile curves with image J software using the conventional angiography as a Ref. [16].

The actual measured profile curves were obtained by setting the square region of interest (ROI) across the CT images at the same position in all three image data sets, reconstructed with FBP, AIDR3D, and FIRST from the 30 patients (Fig. 1a). We placed the square ROI on the main trunk, superficial branch, and deep branch of the cystic artery. The *X*-axis of the square ROI represents distance along the line and the *Y*-axis that is normally wider than one pixel represents the averaged pixel intensity. On the actual measured profile curve, the Δ CT number in three reconstructions was calculated using the formula as below:

$$\Delta\text{CT number} = \text{HU peak} - \text{HU background}(\text{HU}; \text{Hounsfield unit}),$$

where HU peak is the maximum CT number of the profile curve. In addition, we selected the higher CT number of the two curve bases as an HU background to minimize the influence of the fat density (Fig. 1b).

The CT number of the peak and background of the actual measured profile curve was then taken to calculate the normalized profile curve. On the normalized profile curve, we

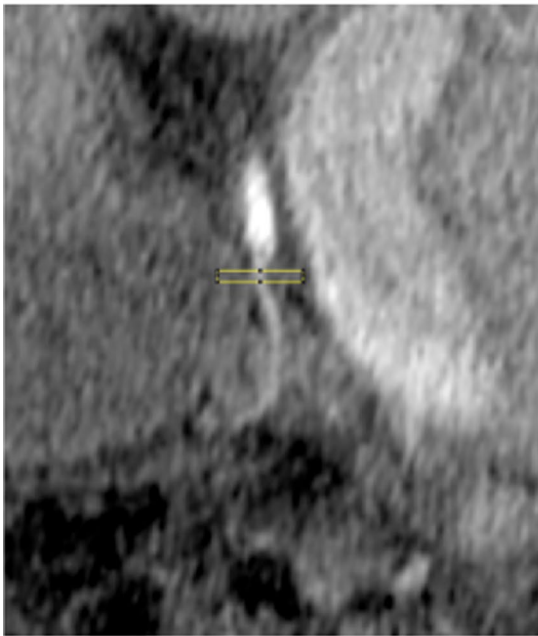
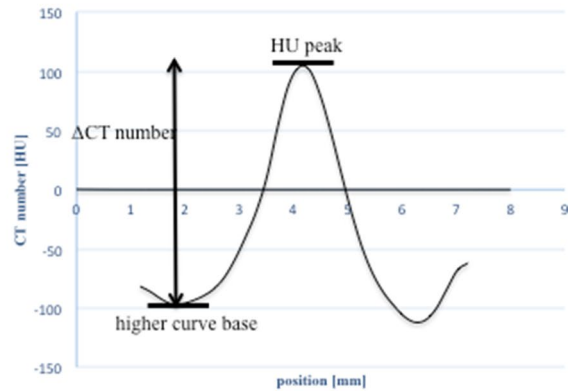
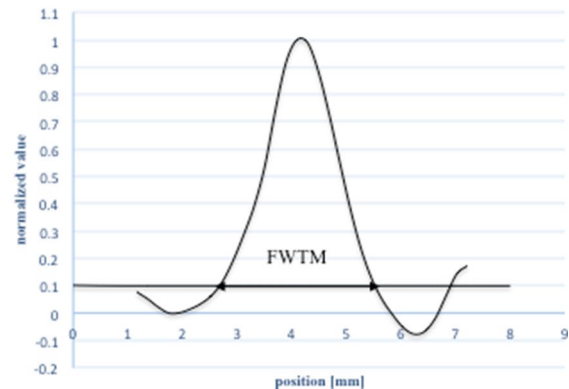
(a) Placement of square region of interest**(b)** The actual measured profile curve**(c)** The normalized profile curve

Fig. 1 **a** Square region of interest (ROI) was placed across CT angiograms (the main trunk, superficial branch, and deep branch of the cystic artery) at the same position in the three image data sets, reconstructed with FBP, AIDR3D, and FIRST. **b** On the actual measured profile curve, the Δ CT numbers in three reconstructions were calcu-

measured the width of the curve one-tenth above the higher base as the full-width at tenth-maximum (FWTM) (Fig. 1c).

Qualitative image analysis

The three image data sets (i.e., FBP, AIDR3D, and FIRST) and the conventional angiography from 30 patients were presented in a random order to two radiologists (K.F. and Y.H., with 9 years of experience and 24 years of experience, respectively). The radiologists were not given access to patient information. CT images were evaluated according to the degree of overall visualization of the cystic artery using a four-point scale. A four-point scale was designed for the image assessment; 1 = poor image quality, obscure origin of cystic artery; 2 = fair image quality, notable blurring of luminal boundaries; 3 = good image quality, minor blurring of luminal boundaries; and 4 = excellent image quality, sharp continuous luminal boundaries at more peripheral branches (Fig. 2).

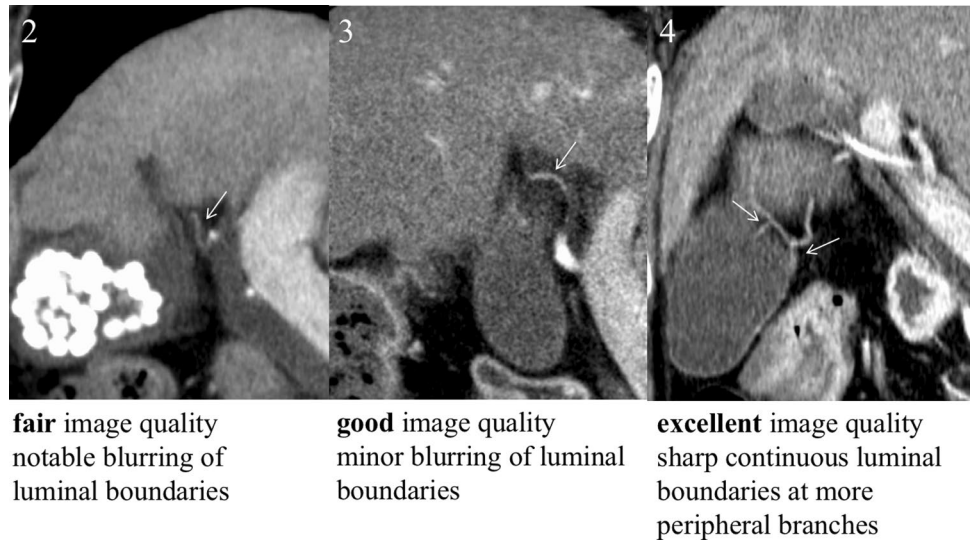
lated from the HU peak and HU background (higher curve base). **c** On the normalized profile curve, we measured the width of the curve one-tenth above the higher base as the full-width at tenth-maximum (FWTM) in the three reconstructions

Statistical analysis

The mean Δ CT number, FWTM, and visualization scores of FIRST were compared with FBP and AIDR3D. Repeated measure analysis of variance followed by post hoc analysis with a holm correction was used. Statistical significance was set at $p < 0.05$. We also examined what part of the cystic arteries had been influenced most by each reconstruction using Cohen's d effect size.

Interobserver agreement for visualization scores was evaluated with the weighted Cohen k test using the following scale: k values of less than 0.20 indicated poor agreement; 0.21–0.40, fair agreement; 0.41–0.60, moderate agreement; 0.61–0.80, good agreement; and 0.81–1.00, excellent agreement.

Fig. 2 Images and text show grading scale for delineation of vessel in CT angiography (CTA). This three (2–4) grade scale is described in text with accompanying image examples. There were no cases corresponding to grade 1 in this study



Results

Quantitative image analysis

The results of quantitative image analysis are summarized in Table 1.

The mean Δ CT number of FIRST in all the areas of the cystic artery was the highest among three reconstructions: the mean Δ CT number of the main trunk; FBP 128.52 ± 56.75 HU, AIDR3D 117.21 ± 56.43 HU, FIRST 159.55 ± 65.83 HU, the mean Δ CT number of the superficial branch; FBP 88.28 ± 39.72 HU, AIDR3D 78.13 ± 37.27 HU, FIRST 111.64 ± 48.29 HU, the mean Δ CT number of the deep branch; FBP 81.20 ± 34.85 HU, AIDR3D 71.65 ± 33.23 HU, FIRST 100.72 ± 43.08 HU, respectively.

The mean Δ CT number of FIRST in all the areas of cystic artery was statistically, significantly better than those of FBP and AIDR3D (the main trunk: FIRST vs. FBP, $p < 0.01$, and FIRST vs. AIDR3D, $p < 0.01$, the superficial branch: FIRST vs. FBP, $p < 0.01$, and FIRST vs. AIDR3D, $p < 0.01$, the deep branch: FIRST vs. FBP, $p < 0.01$, and FIRST vs. AIDR3D, $p < 0.01$, respectively).

Although we calculated the effect size to evaluate the influence of FIRST for the peripheral branches (the superficial branch or the deep branch) and the main trunk of the cystic artery, the superiority of FIRST for the peripheral branches was not shown (Cohen’s d effect size). Figure 3 shows a practical case of profile curves with FBP (a), AIDR3D (b), and FIRST (c) in a 67-year-old man. Figure 3d shows the Δ CT numbers of a main trunk of the cystic artery on an actual measure profile curve. The Δ CT number with FIRST is the highest (FIRST 200.00 HU, FBP 161.67 HU, AIDR3D 159.00 HU).

Table 1 Mean Δ CT numbers (HU) of the main trunk, the superficial branch and the deep branch of the cystic arteries reconstructed with FBP, AIDR3D, and FIRST from the 30 patients

	Main trunk		Superficial branch		Deep branch	
	Δ CT number	HU background	Δ CT number	HU background	Δ CT number	HU background
FBP	128.52 ± 57.83	$116.87 \pm 42.10/2.18 \pm 40.41$	88.28 ± 40.47	$88.53 \pm 33.00/9.96 \pm 35.92$	81.20 ± 35.54	$76.78 \pm 28.99/5.09 \pm 25.84$
AIDR3D	117.21 ± 57.51	$107.75 \pm 38.82/15.00 \pm 40.14$	78.13 ± 37.98	$80.60 \pm 32.73/12.64 \pm 35.43$	71.65 ± 33.89	$70.44 \pm 28.72/8.04 \pm 27.17$
FIRST	159.55 ± 67.08	$135.14 \pm 46.97/-9.56 \pm 38.11$	111.64 ± 49.21	$102.90 \pm 32.98/0.84 \pm 36.59$	100.72 ± 43.93	$90.88 \pm 33.59/2.40 \pm 24.13$
P1	<0.001		<0.001		<0.001	
P2	<0.001		<0.001		<0.001	
P3	<0.001		<0.001		<0.001	

HU Hounsfield unit, FBP filtered back projection, AIDR3D adaptive iterative dose reduction 3D, FIRST forward-projected, model-based, iterative reconstruction solution

P1 = comparison between the FBP and AIDR 3D images

P2 = comparison between the FBP and FIRST images

P3 = comparison between the AIDR 3D and FIRST images

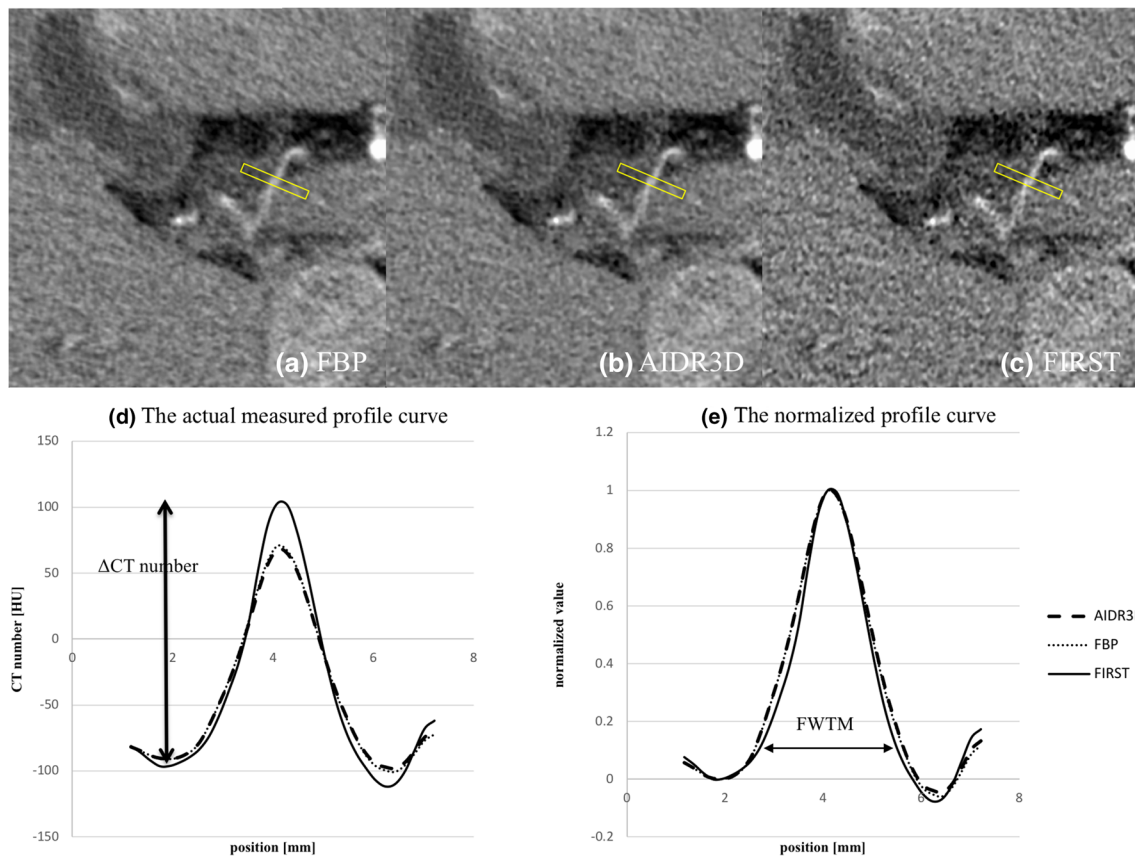


Fig. 3 This figure is a Practical case of profile curves with FBP (a), AIDR3D (b), and FIRST (c) in a 67-year-old man. The square ROI was placed on all three image data sets. Axial CT image with FIRST (c) allows the best visualization of the cystic artery compared to FBP (a) and AIDR3D (b). **d** Δ CT numbers of a main trunk of the cystic

artery on an actual measure profile curve. The Δ CT number with FIRST is the highest (FIRST 200.00 HU, FBP 161.67 HU, AIDR3D 159.00 HU). **e** FWTMs of main trunk of the cystic artery on a normalized profile curve. The FWTM of FIRST that represents the vessel blurring is the smallest (FIRST 2.86, FBP 3.05, AIDR3D 3.07)

Table 2 Mean full-width at one-tenth-maximum (FWTM) of main trunk, superficial branch and deep branch of cystic arteries reconstructed with FBP, AIDR3D, and FIRST from the 30 patients

	Main trunk	Superficial branch	Deep branch
FBP	2.90 ± 1.04	2.23 ± 0.60	2.38 ± 0.77
AIDR3D	2.91 ± 1.03	2.25 ± 0.61	2.38 ± 0.78
FIRST	2.87 ± 1.02	2.21 ± 0.58	2.31 ± 0.72
P1	0.93	0.75	0.90
P2	0.93	0.75	0.52
P3	0.93	0.70	0.52

FBP filtered back projection, AIDR3D adaptive iterative dose reduction 3D, FIRST forward projected, model-based, iterative reconstruction solution

P1= comparison between the FBP and AIDR 3D images

P2= comparison between the FBP and FIRST images

P3= comparison between the AIDR 3D and FIRST images

The FWTM of FIRST in all the areas of the cystic artery was the smallest (Table 2): the FWTM of the main trunk; FBP 2.90 ± 1.04 , AIDR3D 2.91 ± 1.03 , FIRST 2.87 ± 1.02 , the FWTM of the superficial branch; FBP 2.23 ± 0.60 , AIDR3D 2.25 ± 0.61 , FIRST 2.21 ± 0.58 , the FWTM of the deep branch; FBP 2.38 ± 0.77 , AIDR3D 2.38 ± 0.78 , FIRST 2.31 ± 0.72 , respectively. Although it has been considered that the high vessel sharpness and low blurring in FIRST reflected this result, there was no significant difference when compared with other reconstructions. Figure 3e shows the FWTMs of main trunk of the cystic artery on a normalized profile curve. The FWTM of FIRST that represents the vessel blurring is the smallest (FIRST 2.86, FBP 3.05, AIDR3D 3.07).

Qualitative image analysis

The visualization scoring of the main trunk, superficial branch, and deep branch of the cystic artery is summarized in Table 3. The mean visualization score was significantly

Table 3 Mean visualization score for subjective image quality reconstructed with FBP, AIDR3D, and FIRST from the 30 patients

	Reader A	Reader B	Kappa value
FBP	2.7 ± 0.5	2.7 ± 0.5	0.965
AIDR3D	2.4 ± 0.5	2.3 ± 0.4	0.965
FIRST	3.5 ± 0.6	3.7 ± 0.5	0.991
P1	0.001	<0.001	
P2	<0.001	<0.001	
P3	<0.001	<0.001	

FBP filtered back projection, AIDR3D adaptive iterative dose reduction 3D, FIRST forward-projected, model-based, iterative reconstruction solution

P1=comparison between the FBP and AIDR 3D images

P2=comparison between the FBP and FIRST images

P3=comparison between the AIDR 3D and FIRST images

better with FIRST (3.5 ± 0.6 for reader A, 3.7 ± 0.5 for reader B) than those with FBP (2.7 ± 0.5 for reader A, 2.7 ± 0.5 for reader B) and AIDR3D (2.4 ± 0.5 for reader A, 2.3 ± 0.4 for reader B) ($p < 0.05$). Interobserver agreement for the visualization score was excellent among the three reconstructions.

Figure 4 shows coronal CT images of the superficial branch of the cystic artery in an 83-year-old woman with

FBP, AIDR3D, and FIRST (Fig. 4a–c) and 3D maximum intensity projection (MIP) images (Fig. 4d–f: not evaluated in this study) and conventional angiography (Fig. 4g). Coronal CT image and 3D MIP image with FIRST allow the best visualization of the cystic artery compared to FBP and AIDR3D.

Discussion

This study evaluated the ability of three image reconstruction algorithms to resolve small abdominal vessels, such as the cystic arteries validating invasive abdominal angiography. We examined quantitative and qualitative measurements of image quality and depiction. The results indicate improvement in the depiction of small vessel anatomy on images created using FIRST over FBP and AIDR3D supporting the previous studies [10–15].

Previous studies have reported that CT angiography using full IR algorithm might be useful for delineating small vascular structures, such as the head and neck artery, the Adamkiewicz artery, and the coronary artery. Niesten et al. [17] demonstrated that vascular contrast was significantly higher in the circle of Willis with full IR compared to FBP or hybrid IR quantitatively. In addition, Nishida et al. [15]

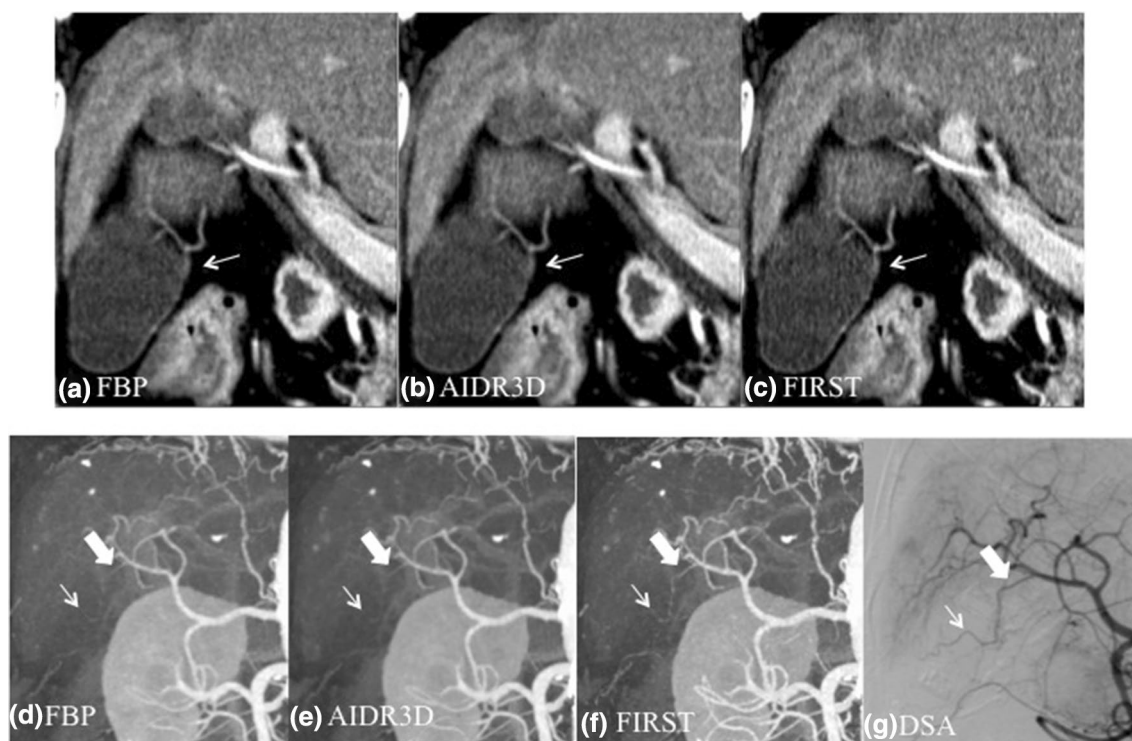


Fig. 4 Coronal CT images of the superficial branch of the cystic artery in an 83-year-old woman with FBP, AIDR3D, and FIRST (Fig. 4a–c) and 3D maximum intensity projection (MIP) images

(Fig. 4d–f) and conventional angiography (Fig. 4g). Coronal CT image and 3D MIP image with FIRST allow the best visualization of the cystic artery compared to FBP and AIDR3D

also showed that full IR has a substantial advantage over FBP and hybrid IR in visualizing the Adamkiewicz artery for both quantitative and qualitative analyses. A few previous reports evaluated the abdominal arteries. Koc et al. [18] demonstrated that full IR improved depiction of the pulmonary artery, hepatic, splenic, and renal artery with decreased image noise, in a pediatric patient population. Recently, Wu et al. [19] reported that FIRST reconstruction algorithm could improve image quality and provide better delineation of proximal abdominal artery structures. However, they did not validate the results using invasive angiography or evaluate the small diameter arteries qualitatively.

The improvement in vessel depiction with FIRST is largely attributable to the increased spatial resolution compared with other reconstruction techniques [14, 20]. FIRST is a model-based reconstruction that repeats both backward and forward processes according to a statistical metric from a raw data set without an initial FBP reconstruction [21]. These forward-projected data are compared with the actual measured data according to statistical metrics, and the computed difference is itself back projected to create an image update. With FIRST algorithm, image noise can be reduced by combining many more iterations with the more complex mathematics. This algorithm includes mathematical recognition models, such as the cone-shape of the X-ray beam in CT, the non-linear polychromatic nature of X-ray beams, the shape considerations of the focal spot and the detectors (optics model). With incorporation of system optics and anatomical information from several mathematical models, we can expect improvements in spatial resolution [21].

However, with FIRST algorithm, it is difficult to adequately characterize the image quality with traditional physical metrics [22], and proper measurement methods are not yet established [23]. Unlike FBP algorithms that exhibit a linear behavior, FIRST algorithm is non-linear and their spatial resolution varies with the object contrast and noise level [24]. We used the profile curve method for quantitative measurements. We believe that this method provides a better analysis compared to CNR, due to the fact that this method can assess the CT number without the influence of image noise. Furthermore, the vessel sharpness and blurring can be evaluated using FWTM. It has been reported that FWTM could describe the sharpness mathematically among different reconstruction methods [25].

Proper identification of cystic arteries allows the avoidance of embolization or accidental injury that not only supply the gallbladder, but also are important for liver vascularization [4]. For the introduction of TACE and LC, we concluded that CT angiography using FIRST algorithm is a practical tool for delineating cystic arteries.

This study has several limitations. First, the sample size was relatively small. Previous angiography, as the reference in this study, made it difficult to increase the sample size.

Thus, further work should be done to support and validate this data. Second, although the image sets used different reconstruction techniques and were presented in a random order, FIRST, AIDR3D, and FBP could be distinguished due to their image appearance. The distinction between FIRST AIDR3D and FBP images may have influenced the interpretation on the results. Third, we did not evaluate the CTA visualization of the cystic artery using low-dose CT, as this study was evaluated retrospectively.

In conclusion, the use of the FIRST algorithm led to improved CTA visualization of the cystic artery when compared with the use of FBP and AIDR3D.

Compliance with ethical standards

Conflict of interest The authors declare that they have no conflict of interest.

Ethical statement All applicable institutional and national guidelines for the care and use of animals were followed.

Informed consent The study was approved by our institutional review board, and the requirement for informed consent had been waived.

References

- Halvorsen JF, Myking AO. The arterial supply and venous drainage of the gall-bladder. A study of one hundred autopsies. *Acta Chir Scand.* 1971;137:659–64.
- Hugh TB, Kelly MD, Li B. Laparoscopic anatomy of the cystic artery. *Am J Surg.* 1992;163:593–5.
- Malagari K, Pomoni M, Spyridopoulos TN, Moschouris H, Kelekis A, Dourakis S, et al. Safety profile of sequential transcatheter chemoembolization with DC bead TM: results of 237 hepatocellular carcinoma (HCC) patients. *Cardiovasc Intervent Radiol.* 2011;34:774–85.
- Torres K, Chrościcki A, Golonka A, Torres A, Staśkiewicz G, Palczak R, et al. The course of the cystic artery during laparoscopic cholecystectomy. *Folia Morphol.* 2009;68(3):140–3.
- Ding YM, Wang B, Wang WX, Wang P, Yan JS. New classification of the anatomic variations of cystic artery during laparoscopic cholecystectomy. *World J Gastroenterol.* 2007;13(42):5629–34.
- Padole A, Ali Khawaja RD, Kalra M, Singh S. CT radiation dose and iterative reconstruction techniques. *AJR.* 2015;204:384–92.
- Den Harder AM, Willeminck MJ, De Ruitter QM, De Jong PA, Schiham AM, Krestin GP, et al. Dose reduction with iterative reconstruction for coronary CT angiography: a systematic review and meta-analysis. *Br J Radiol.* 2016;89:20150068.
- Leipsic JL, Heilbron BG, Hague C. Iterative reconstruction for coronary CT angiography: finding its way. *Int J Cardiovasc Imaging.* 2012;28:613–20.
- Den Harder AM, Willeminck MJ, De Ruitter QM, Schiham AM, Krestin GP, Leiner T, et al. Achievable dose reduction using iterative reconstruction for chest computed tomography: a systematic review. *Eur J Radiol.* 2015;84:2307–13.
- Maeda E, Tomizawa N, Kanno S, Yasaka K, Kubo T, Ino K, et al. The feasibility of forward-projected model-based iterative reconstruction solution (FIRST) for coronary 320-row computed

- tomography angiography: a pilot study. *J Cardiovasc Comput Tomogr*. 2017;11(1):40–5.
11. Ohno Y, Yaguchi A, Okazaki T, Aoyagi K, Yamagata H, Sugihara N, et al. Comparative evaluation of newly developed model-based and commercially available hybrid-type iterative reconstruction methods and filter back projection method in terms of accuracy of computer-aided volumetry (CADv) for low-dose CT protocols in phantom study. *Eur J Radiol*. 2016;85(8):1375–82.
 12. Tatsugami F, Higaki T, Sakane H, Fukumoto W, Kaichi Y, Iida M, et al. Coronary artery stent evaluation with model-based iterative reconstruction at coronary CT angiography. *Acad Radiol*. 2017;24(8):975–81.
 13. Scheffel H, Stolzmann P, Schlett CL, Engel LC, Major GP, Károlyi M, et al. Coronary artery plaques: cardiac CT with model-based and adaptive-statistical iterative reconstruction technique. *Eur J Radiol*. 2012;81(3):e363–9.
 14. Katsura M, Matsuda I, Akahane M, Sato J, Akai H, Yasaka K, et al. Model-based iterative reconstruction technique for radiation dose reduction in chest CT: comparison with the adaptive statistical iterative reconstruction technique. *Eur Radiol*. 2012;22(8):1613–23.
 15. Nishida J, Kitagawa K, Nagata M, Yamazaki A, Nagasawa N, Sakuma H. Model-based iterative reconstruction for MultiDetector row CT assessment of the adamkiewicz artery. *Radiology*. 2014;270(1):282–91.
 16. Tsukada J, Yamada M, Yamada Y, Yamazaki S, Imanishi N, Tamura K, et al. Comparison of the diagnostic accuracy of FBP, ASiR, and MBIR reconstruction during CT angiography in the evaluation of a vessel phantom with calcified stenosis in a distal superficial femoral artery in a cadaver extremity. *Medicine*. 2016;95(27):e4127.
 17. Niesten JM, van der Schaaf IC, Vos PC, Willemink MJ, Velthuis BK. Improving head and neck CTA with hybrid and model-based iterative reconstruction techniques. *Clin Radiol*. 2015;70:1252–9.
 18. Koc G, Courtier JL, Phelps A, Marcovici PA, MacKenzie JD. Computed tomography depiction of small pediatric vessels with model-based iterative reconstruction. *Pediatr Radiol*. 2014;44:787–94.
 19. Wu R, Hori M, Onishi H, Nakamoto A, Fukui H, Ota T, et al. Effects of reconstruction technique on the quality of abdominal CT angiography: a comparison between forward projected model-based iterative reconstruction solution (FIRST) and conventional reconstruction methods. *Eur J Radiol*. 2018;106:100–5.
 20. Thibault JB, Sauer KD, Bouman CA, Hsieh J. A three-dimensional statistical approach to improved image quality for multislice helical CT. *Med Phys*. 2007;34:4526–44.
 21. Shuman WP, Green DE, Busey JM, Kolokythas O, Mitsumori LM, Koprowicz KM, et al. Model-based iterative reconstruction versus adaptive statistical iterative reconstruction and filtered back projection in liver 64-MDCT: focal lesion detection, lesion conspicuity, and image noise. *AJR Am J Roentgenol*. 2013;200(5):1071–6.
 22. McCollough CH, Chen GH, Kalender W, Leng S, Samei E, Taguchi K, et al. Achieving routine submillisievert CT scanning: report from the summit on management of radiation dose in CT. *Radiology*. 2012;264:567–80.
 23. Mori I. Non-linear nature of recent CT images and image quality evaluation. 2013. <http://hdl.handle.net/10097/55355>. Accessed 31 Jan 2013.
 24. Oda S, Weissman G, Vembar M, Weigold WG. Iterative model reconstruction: improved image quality of low-tube-voltage prospective ECG-gated coronary CT angiography images at 256-slice CT. *Eur J Radiol*. 2014;83(3):1408–15.
 25. Gordic S, Desbiolles L, Sedlmair M, Manka R, Plass A, Schmidt B, et al. Optimizing radiation dose by using advanced modelled iterative reconstruction in high-pitch coronary CT angiography. *Eur Radiol*. 2016;26:459–68.

Publisher's Note Springer Nature remains neutral with regard to jurisdictional claims in published maps and institutional affiliations.